

Perspective

Self-Trapped Excitons in All-Inorganic Halide Perovskites: Fundamentals, Status and Potential Application

Shunran Li, Jiajun Luo, Jing Liu, and Jiang Tang

J. Phys. Chem. Lett., **Just Accepted Manuscript** • DOI: 10.1021/acs.jpcllett.8b03604 • Publication Date (Web): 04 Apr 2019

Downloaded from <http://pubs.acs.org> on April 5, 2019

Just Accepted

“Just Accepted” manuscripts have been peer-reviewed and accepted for publication. They are posted online prior to technical editing, formatting for publication and author proofing. The American Chemical Society provides “Just Accepted” as a service to the research community to expedite the dissemination of scientific material as soon as possible after acceptance. “Just Accepted” manuscripts appear in full in PDF format accompanied by an HTML abstract. “Just Accepted” manuscripts have been fully peer reviewed, but should not be considered the official version of record. They are citable by the Digital Object Identifier (DOI®). “Just Accepted” is an optional service offered to authors. Therefore, the “Just Accepted” Web site may not include all articles that will be published in the journal. After a manuscript is technically edited and formatted, it will be removed from the “Just Accepted” Web site and published as an ASAP article. Note that technical editing may introduce minor changes to the manuscript text and/or graphics which could affect content, and all legal disclaimers and ethical guidelines that apply to the journal pertain. ACS cannot be held responsible for errors or consequences arising from the use of information contained in these “Just Accepted” manuscripts.

1
2
3
4
5
6
7 **Self-trapped Excitons in All-inorganic Halide**
8
9
10
11 **Perovskites: Fundamentals, Status and Potential**
12
13
14
15 **Application**
16
17
18
19

20 *Shunran Li^{†,‡}, Jiajun Luo^{†,‡}, Jing Liu, [†] Jiang Tang^{*,†}*
21
22
23
24

25 [†]Sargent Joint Research Center, Wuhan National Laboratory for Optoelectronics
26
27
28 (WNLO) and School of Optical and Electronic Information, Huazhong University
29
30
31 of Science and Technology (HUST), Wuhan 430074, China
32
33
34
35

36 [‡] These authors contribute equally to this paper.
37
38
39

40 **Corresponding Author**
41
42
43

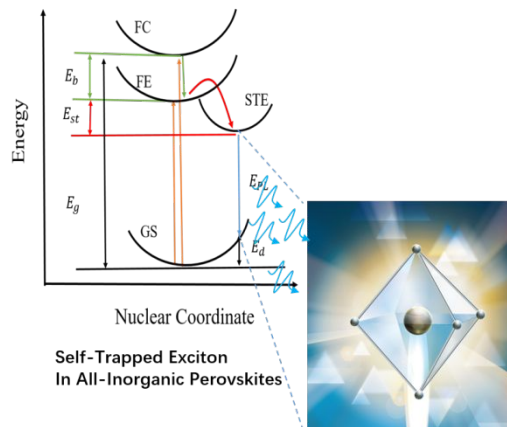
44 *E-mail: jtang@mail.hust.edu.cn (J.T)
45
46
47
48

49 **ABSTRACT:** Photoluminescence is a radiative recombination process of electron
50
51
52 hole pairs. Self-trapped exciton (STE), occurring in a material with soft lattice
53
54
55 and strong electron-phonon coupling, emits photons with broad spectrum and
56
57
58
59
60

1
2
3 large stokes-shift. Recently, series halide perovskites with efficient STE
4
5
6
7 emission have been reported and showed promise for solid state lighting. In
8
9
10 this Perspective, we present an overview of various photoluminescence with the
11
12
13 emphasis on the mechanism and characteristics of emission derived from STE.
14
15
16
17 This is followed by the introduction of STE emission in hybrid halide
18
19
20 perovskites. We then introduce all-inorganic STE emitters and focus in particular
21
22
23 on the mechanism of STE in double perovskite $\text{Cs}_2\text{AgInCl}_6$ and strategies for
24
25
26 efficiency improvement. Last we summarize the current photoluminescence and
27
28
29 electroluminescence applications of STE emitters as well as the potential in
30
31
32
33 luminescent solar concentrators, and overlook future research opportunities.
34
35
36
37
38
39

40 TOC GRAPHICS

41
42
43
44
45
46
47
48
49
50
51
52
53
54
55
56
57
58
59
60



KEYWORDS: self-trapped exciton, lead-free perovskite, low dimension, large stokes-shift, broad spectrum.

Photoluminescence (PL) is a basic and important property of semiconductors. There are two types of electronic transitions accompanied with photoluminescence in solids: intrinsic photoluminescence and extrinsic photoluminescence.¹ Intrinsic photoluminescence can be further divided into band-to-band luminescence, exciton luminescence and cross luminescence. Extrinsic luminescence further comprises unlocalized type, such as donor-acceptor pair luminescence as well as luminescence caused by isoelectronic trap, and localized type like ionoluminescence and defect luminescence.¹

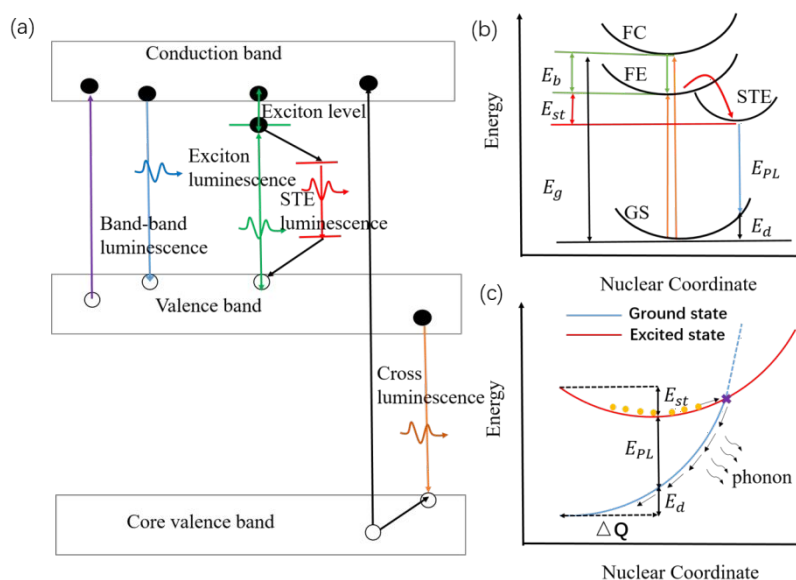


Figure 1. (a) Schematic of various intrinsic photoluminescence, including band-to-band luminescence, exciton luminescence, STE luminescence as well as cross luminescence. (b) Schematic of the energy level structure of STE (GS = ground state, FE = free exciton state, FC = free carrier state, STE = self-trapped exciton state, E_g = bandgap energy, E_b = exciton binding energy, E_{st} = self-trapping energy, E_d = lattice deformation energy, E_{PL} = emission energy). (c) Schematic of the nonradiative recombination process for STE when S is large. Orange circles represent excited electrons.

1
2
3
4 As shown in Figure 1a, band-to-band luminescence indicates that
5
6
7 electrons in the conduction band recombine with holes in the valence band.
8
9
10 The emission of mainstream light-emitting-diodes belongs to band-to-band
11
12
13 luminescence². Cross luminescence will appear when an electron in the valence
14
15
16 band and a hole in the core band recombine. This kind of luminescence is
17
18
19 often observed in alkali halides and alkaline-earth halides, and owing to the
20
21
22 fast recombination time (even <1 ns)³, it plays a crucial role in fast scintillators.
23
24
25
26
27 Exciton luminescence means that an electron and a hole attract each other by
28
29
30 Coulomb interaction and then recombine, emitting a photon. For semiconductors
31
32
33 with low exciton binding energy, exciton luminescence can only be observed at
34
35
36 low temperature as excitons will convert to free carriers with the aid of thermal
37
38
39 energy at room temperature. The exciton emission energy is normally slightly
40
41
42 lower than the bandgap by the exciton binding energy, but there is an unusual
43
44
45 kind of exciton, called self-trapped exciton (STE), whose emission energy is
46
47
48 much smaller than the bandgap^{1, 4}.
49
50
51
52
53
54
55
56
57
58
59
60

1
2
3
4 STEs widely exist in halide crystals⁵⁻⁶, condensed rare gases⁷, organic
5
6
7 molecular crystals⁸. In these solids, electron-phonon interactions are strong
8
9
10 enough for excited electrons and holes to cause elastic distortions in the lattice
11
12
13 surrounding them. Thus once electrons and holes are photo-generated, they will
14
15
16 be quickly self-trapped because the self-trapped state is more stable than the
17
18
19 one in which they would move, dragging the lattice distortion. For example, in
20
21
22 alkali halides photo-generated holes are self-trapped by two adjacent halogen
23
24
25 ions approaching one another. This molecular ion type center X_2^- is called a V_k
26
27 center and eventually emits intrinsic luminescence when further captures an
28
29
30 electron⁵. In the process of STE, exciton will lose some energy, called self-
31
32
33 trapping energy E_{st} . At the same time the energy of ground state will rise due
34
35
36 to lattice deformation, and the increased energy is called lattice deformation
37
38
39 energy E_d . Consequently, the emission energy can be described by $E_{PL} = E_g - E_{st} -$
40
41
42 E_d (Figure 1b), which is the origin of the large stokes-shift in STE emission.
43
44
45
46
47
48
49
50

51 Extrinsic luminescence is also very common for many practical
52
53
54 photoluminescence applications. The mechanism of most phosphors belongs to
55
56
57
58
59
60

1
2
3 extrinsic luminescence. For instance, green phosphor ZnS with Cu,Al doping is
4
5
6
7 a typical donor-acceptor pair luminescence material⁹. Green light-emitting diode
8
9
10 GaP with N isoelectronic doping and red light-emitting diode GaP with Zn-O
11
12
13 isoelectronic doping are representative isoelectronic trap luminescence, which
14
15
16
17 were widely applied to the market before the breakthrough of InGaN and
18
19
20 AlGaInP light-emitting diodes². Ionoluminescence is also one important sort of
21
22
23
24 extrinsic luminescence, as exhibited in rare earth ions. Rare earth ions are
25
26
27 famous for their efficient and stable luminescence with tunable and generally
28
29
30 broad spectrum depending on the host lattice, which is necessary for high
31
32
33
34 quality phosphor used in general lighting.

35
36
37
38 However, in view of the scarcity of rare earth resources and the
39
40
41 importance of rare earth element to high-performance magnets, catalysts, alloys,
42
43
44 glasses, and electronics, it is highly significant to develop high performance
45
46
47 rare-earth free phosphors. In particular, single-source phosphors with white
48
49
50
51 emission not only avoid the self-absorption and color instability problems
52
53
54
55 associated with the current method of combining multiple phosphors for white
56
57
58
59
60

1
2
3 emission, but also simplifies the fabrication procedure Broadband and white
4
5
6 emission (full width at half maximum, $FWHM > 100$ nm, covering the entire
7
8
9 visible spectrum) emitters are extremely rare for most intrinsic luminescence.
10
11
12 Encouragingly, STE emission generally features broad spectrum. As mentioned
13
14 before, strong electron-phonon coupling is essential for the STE formation,
15
16
17 which is evaluated by the well-known Huang-Rhys factor S .⁴ The electron-
18
19
20 phonon coupling has a strong connection with the $FWHM$ of luminescence, as
21
22
23 described by the equation¹⁰:
24
25
26
27
28
29
30

$$FWHM = 2.36 \sqrt{S} \hbar \omega_{phonon} \sqrt{\coth \frac{\hbar \omega_{phonon}}{2k_b T}} \quad (1)$$

31
32
33
34
35
36 Where \hbar is reduced Planck constant, ω_{phonon} is phonon frequency, T is
37
38
39 temperature, and k_b is Boltzmann constant, respectively. In principle, S can be
40
41
42 obtained by fitting the temperature dependent $FWHM$ of PL peaks with the
43
44
45 equation above. Although there is no absolute functional relation between the
46
47
48 existence of STE and the value of S , it is certain that the larger S value is,
49
50
51
52
53 the more likely STE forms. On the other hand, the coordinate difference
54
55
56
57
58
59
60

1
2
3 between the free-exciton and STE configurations, ΔQ has positive correlation
4
5
6 with S .⁴ An overly large S can bring us a broad emission but also lead to the
7
8
9 tendency for the excited- and ground-state curves to cross in the configuration
10
11
12 coordinate diagram, which means that some excited electrons and holes can
13
14
15 recombine via this interaction non-radiatively, emitting several phonons (Figure
16
17
18
19
20
21
22
23
24
25
26
27
28
29
30
31
32
33
34
35
36
37
38
39
40
41
42
43
44
45
46
47
48
49
50
51
52
53
54
55
56
57
58
59
60

1c). Thereby, S should be a suitable value, neither too big nor too small to achieve an efficient STE emission.

Since 2014, a number of halide perovskites have been found to emit abnormally broad spectra with a strength visible to naked eyes.¹¹⁻²⁰ Through the replacement of A-site and X-site elements the spectrum can be continuously adjusted from cold-white to warm-white. This kind of perovskites with great potential lighting applications have aroused wide attention and further researches indicated that STE is responsible for the unique emission.²¹⁻²³ It is worth noting that several all-inorganic perovskites with excellent STE emitting were reported recently.²⁴⁻²⁶ In this Perspective, we will overview the basic property of organic halide perovskites with STE emission. We will then highlight

the milestones achieved in the optical property and the mechanism of the lead-free all-inorganic perovskites with efficient STE emission. Finally, we will discuss the photoluminescence and electroluminescence (EL) based applications of all-inorganic lead-free perovskites with STE emission as well as future research opportunities.

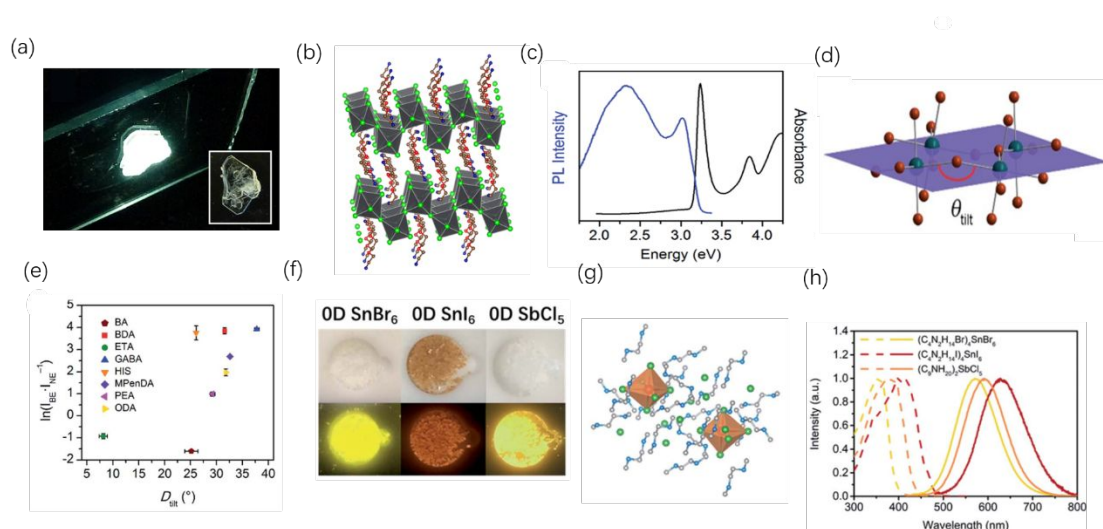


Figure 2. (a) The photograph of (EDBE)[PbBr₄] under 365nm light, inset shows the perovskite under ambient light (EDBE = 2,2'-(ethylenedioxy)bis(ethylammonium)). Reprinted with permission from ref 15.

Copyright 2014 American Chemical Society. (b) X-ray structure of (EDBE)[PbBr₄]: gray, green, red, brown, blue represent Pb, Br, O, C and N atoms. H atoms

1
2
3 are omitted for clarity. (c) Absorption (black) and emission (blue) for
4
5
6 (AEA)PbBr₄ (AEA = 3-(2-ammonioethyl)anilinium). (d) Schematic of
7
8
9
10 interoctahedral tilting θ_{tilt} in a single Pb-Br layer. (e) Values of $\ln(I_{BE}/I_{NE})$ for
11
12
13 various layered lead halide perovskites as a function of interoctahedral tilting θ_{tilt}
14
15
16 . D_{tilt} represents $180^\circ - \theta_{tilt}$; BE and NE represent broad emission and narrow
17
18
19
20 emission in layered perovskites. Panels c-e are reprinted with permission from
21
22
23 ref 22. Copyright 2017 American Chemical Society. (f) The photograph of 0D
24
25
26 tin and antimony perovskites under ambient light and 365nm light. (g) Crystal
27
28
29 structure of (C₄N₂H₁₄Br)₄SnBr₆: red, green, blue, gray represent Sn, Br, N, C
30
31
32 atoms; H atoms are hidden for clarity. (h) PL and PLE of (C₄N₂H₁₄Br)₄SnBr₆,
33
34
35 (C₄N₂H₁₄I)₄SnI₆, (C₉NH₂₀)₂SbCl₅. Panels f-h are reprinted with permission from
36
37
38
39
40
41 ref 19 published by The Royal Society of Chemistry.
42
43
44
45
46
47
48

49 Karunadasa et al. and Kanatzidis et al. first reported several low
50
51
52
53 dimensional lead halide perovskites with intrinsic broadband emission from 400
54
55
56
57
58
59
60

1
2
3 nm to 800 nm, covering the visible region, such as (N-MEDA)[PbBr_{4-x}Cl_x] (N-
4
5
6
7 MEDA = N-methylethane-1,2-diammonium, $x = 0 \sim 1.2$), EA₄Pb₃Cl_{10-x}Br_x (EA =
8
9
10 ethylammonium, $x < 10$) (Figure 2a).^{14-16, 18, 21-23} All of them include a large
11
12
13 organic group at A-site and further form a two-dimensional (2D) structure
14
15
16 (Figure 2b). Thus compared with three-dimensional (3D) perovskites they all
17
18
19 have an obvious exciton absorption peak (Figure 2c). Please note that in this
20
21
22
23
24 Perspective, all the perovskite dimension refers to the connection of octahedron
25
26
27 instead of material size. Due to the large organic groups and the mixed halides
28
29
30 in some cases, the lead octahedra and the inorganic frameworks show
31
32
33
34 distortions to some degree, which can be describe by the interoctahedral tilting
35
36
37 θ_{tilt} (Figure 2d).^{14, 18} The STE property depends profoundly on the inorganic
38
39
40 structure distortion. Besides, further research showed that there exists a
41
42
43
44 potential barrier for self-trapping in two dimensional systems, which could allow
45
46
47 some excited carriers to recombine as free exciton (FE) luminescence rather
48
49
50 than STE luminescence.²¹ The emission spectra of 2D perovskites usually
51
52
53
54 comprise two peaks (Figure 2c): the main broad emission with lower energy is
55
56
57
58
59
60

1
2
3 STE luminescence and the secondary narrow emission with higher energy is
4
5
6 FE luminescence. The ratio of FE luminescence and STE luminescence is also
7
8
9
10 dependent on the distortion (Figure 2e).²³ A warm-white STE luminescence and
11
12
13 a blue FE luminescence constitute a standard white emission. Thus, white-light
14
15
16 emitter can be designed with appropriate A-site organic group²³. But as
17
18
19 mentioned before, large S, and probably some deep defects in those
20
21
22
23 perovskites results in a low emission efficiency. The highest PLQY in lead
24
25
26 halide perovskites with white emission is 9% in (EDBE)PbBr₄.²³ For the detailed
27
28
29 discussion on STE in this type of materials, readers are encouraged to refer to
30
31
32
33 the excellent review written by Prof. Karunadasa.²³
34
35
36
37

38 In parallel, Ma et al. and Ning et al. reported a series of lead-free tin
39
40
41 and antimony perovskites with broadband emission and especially a near unity
42
43
44 photoluminescence quantum yield (PLQY), which have outstanding efficiency
45
46
47 and avoid the environmental issues caused by Pb (Figure 2f).^{13, 17, 19-20, 27} For
48
49
50 those perovskites, the B-site element is small while the A-site component is
51
52
53
54 large in volume. Therefore the [SnBr₆]⁴⁻ or [SbCl₅]²⁻ is totally isolated by the
55
56
57
58
59
60

1
2
3 large organic group, forming so-called 0D structure (Figure 2g). Photogenerated
4
5
6 carriers are confined in these isolated octahedral, experiencing strong quantum
7
8
9 confinement and hence enjoying high PLQY. In 0D systems, there is no inter-
10
11
12 connected inorganic framework and hence no conception of interoctahedral
13
14
15
16 tilting which plays a significant role in the emission of 2D lead halide
17
18
19 perovskites.²² Thus the STE property depends mainly on the distortion in a
20
21
22 single octahedron and the octahedral composition. The energy barrier between
23
24
25
26
27 FE and STE is believed not to exist in 0D materials.²⁸⁻³⁰ This is probably
28
29
30 because the immediate distortion of the more mobile $[\text{SnBr}_6]^{4-}$ or $[\text{SbCl}_5]^{2-}$
31
32
33 octahedra, leading to sole STE emission. Therefore contrast to 2D lead halide
34
35
36 perovskites with STE emission discussed above, these 0D lead-free perovskite
37
38
39 have high emission efficiency but a narrower emission with very good Gaussian
40
41
42 shape (Figure 2h) because of the absence of FE emission.¹⁹ The
43
44
45
46 disappearance of FE luminescence means that 0D perovskites are capable to
47
48
49
50 own warm-white emission at most unless the FWHM of STE emission is larger
51
52
53 than 250 nm, which is at the expense of PLQY and unworthy.
54
55
56
57
58
59
60

1
2
3
4 STE formation is believed to have a strong relationship with the
5
6
7 dimensionality of the system.^{21, 28-32} In other words, a large electron-phonon
8
9
10 coupling is crucial to the formation of STE, and the low crystal dimensionality
11
12
13 can facilitate octahedral distortion and STE formation, as well as high emission
14
15
16 efficiency because of the strong quantum confinement particularly in the 0D
17
18
19 perovskites. Despite diverse organo-ammonium cations are available for A site,
20
21
22 their moisture and thermal instability restricts practical applications. Thereby, all-
23
24
25 inorganic perovskites are proposed as a promising alternative considering their
26
27
28
29
30 excellent stability.
31
32
33
34
35
36
37
38
39
40
41
42
43
44
45
46
47
48
49
50
51
52
53
54
55
56
57
58
59
60

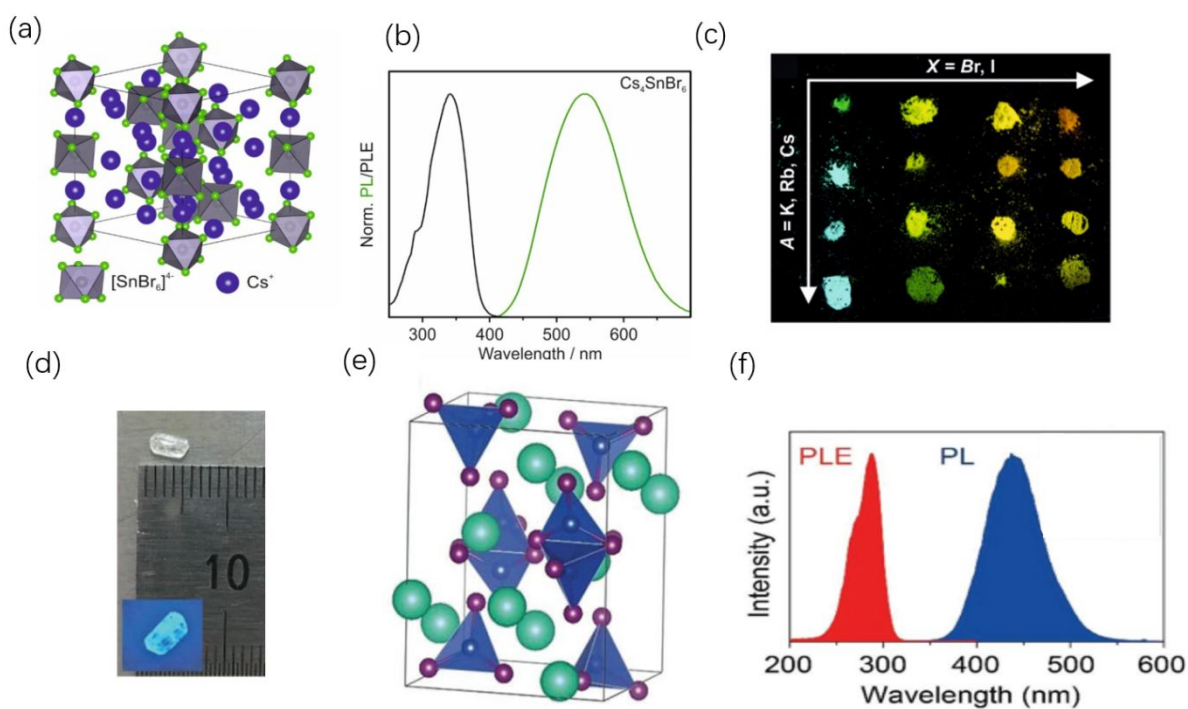


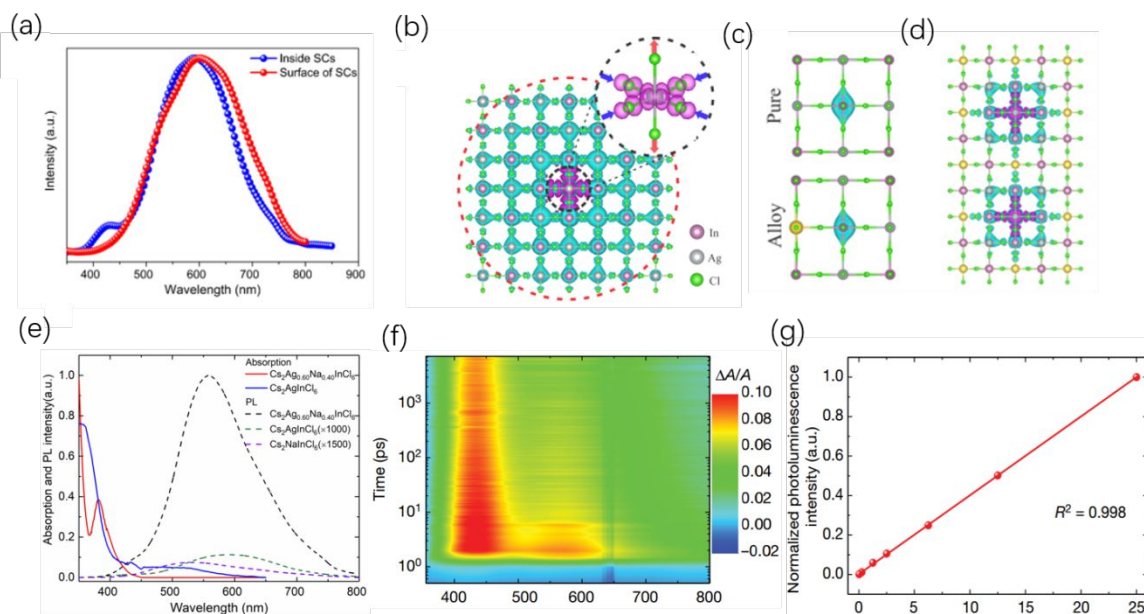
Figure 3. (a) Crystal structure of Cs_4SnBr_6 , grey, green and violet represent Sn, Br and Cs atoms. (b) The PL and PLE of Cs_4SnBr_6 . (c) The photograph of $\text{Cs}_{4-x}\text{A}_x\text{Sn}(\text{Br}_{1-y}\text{I}_y)_6$ ($\text{A}=\text{K}, \text{Rb}$) under 365nm light. Panels a-c are reprinted from ref 24 with permission from John Wiley & Sons Ltd. (d) The photograph of $\text{Cs}_3\text{Cu}_2\text{I}_5$ crystal under ambient light, inset shows the crystal under 245nm light. (e) Crystal structure of $\text{Cs}_3\text{Cu}_2\text{I}_5$, blue, violet and cyan represent Cu, I, Cs atoms. (f) The photoluminescence (PL) and photoluminescence excitation (PLE) of $\text{Cs}_3\text{Cu}_2\text{I}_5$. Panels d-f are reprinted from ref 25 with permission from John Wiley & Sons Ltd.

1
2
3
4
5
6
7
8 In 3D all-inorganic perovskite with crystal structure of cubic phase ABX_3 ,
9
10
11 crystal lattice is difficult to distort because octahedra connect with each other
12
13
14 via vertex firmly. Even formed, the STE is unstable.³³ As discussed before, a
15
16
17 reduced dimensionality and localized electrons and holes contribute to the
18
19
20 formation of efficient STE. For example, yellow orthorhombic phase $CsPbI_3$ is a
21
22
23 kind of low dimensional inorganic perovskite and thus STEs emission was
24
25
26 observed.³⁴ Recently Kovalenko et al. reported 0D material Cs_4SnBr_6 with a
27
28
29 relatively high PLQY ($\sim 15\%$).²⁴ From the perspective of crystal structure,
30
31
32 $[SnBr_6]^{4-}$ octahedron is separated by Cs^+ ions totally (Figure 3a). The optical
33
34
35 property is also a typical STE emission: large stokes-shift and broad spectrum
36
37
38 (Figure 3b). Simulation showed Jahn-Teller distortion in $[SnBr_6]^{4-}$ is the origin of
39
40
41 STE.²⁴ Compared with those hybrid tin 0D perovskites discussed above, the
42
43
44 emission spectrum is slightly broader but PLQY is obviously lower. However,
45
46
47 the moisture and thermal stability of Cs_4SnBr_6 is significantly enhanced because
48
49
50 of the absence of organic group. Another superiority of Cs_4SnBr_6 is the optical
51
52
53
54
55
56
57
58
59
60

1
2
3 property can be adjusted continuously by substituting A site with K^+ or Rb^+ and
4
5
6 X site with I^- (Figure 3c).²⁴ But the frangibility to oxidation of Sn^{2+} remains a
7
8
9
10 significant concern for long-term stability. Thus it is meaningful to find more
11
12
13 stable and efficient all-inorganic STE emitter.
14
15
16
17

18 Hosono et al. reported a nontoxic all-inorganic halide 0D material
19
20
21 $Cs_3Cu_2I_5$ with efficient broad blue emission (PLQY up to 90%) (Figure 3d).²⁵
22
23
24 Similarly, the emission center, $[Cu_2I_5]^{3-}$, is isolated with each other by Cs^+ in
25
26
27 $Cs_3Cu_2I_5$ (Figure 3e). Thus excitons are spatially confined around emission
28
29
30 centers, favoring the radiative recombination and contributing a high PLQY. In
31
32
33
34 addition, the efficient blue emission spectrum of $Cs_3Cu_2I_5$ is comparatively
35
36
37 narrow among perovskites with STE emission (Figure 3f), which is also rare
38
39
40 and of great value. Furthermore, Cu^+ is thermodynamically stable and more
41
42
43 anti-oxidative contrast to Sn^{2+} ; however its moisture stability could still be a
44
45
46 concern. The ideal STE emitter should combine a near-unity PLQY with an
47
48
49 excellent air, light and thermal stability, and preferably white emission as for
50
51
52 solid state lighting applications. Double perovskites emerged as the potential
53
54
55
56
57
58
59
60

1
2
3 substitute for lead halide perovskites.³⁵⁻⁴⁴ The elements making up double
4
5
6
7 perovskites are Ag^+ , Bi^{3+} and In^{3+} etc.^{37, 40, 42} Those elements generally have
8
9
10 fixed chemical valence, ensuring better stability. Moreover, recent study
11
12
13 indicated that despite the 3D structural dimensionality of double perovskites,
14
15
16
17 many of them have a 0 D electronic dimensionality, which is a shortcoming for
18
19
20 solar cell absorbers but a merit for STE emitter.^{35, 45}
21
22
23
24
25
26
27
28



51 **Figure 4.** (a) The PL spectrum of $\text{Cs}_2\text{AgInCl}_6$ single crystals (SCs). Reprinted
52
53
54 from ref ⁴⁶. Copyright 2017 American Chemical Society. (b) STE in $\text{Cs}_2\text{AgInCl}_6$.
55
56
57
58
59
60

1
2
3 The cyan and magenta isosurfaces represent the electron states and the hole
4 states. Inset shows the Jahn-Teller distortion of the $[\text{AgCl}_6]$ octahedron. (c) The
5 parity change of electron wave function (isosurface at Ag atom) of STE
6 between $\text{Cs}_2\text{AgInCl}_6$ and $\text{Cs}_2\text{Na}_x\text{Ag}_{1-x}\text{InCl}_6$. (d) The confined STE in $\text{Cs}_2\text{Na}_x\text{Ag}_{1-x}$
7 InCl_6 . (e) The absorption and photoluminescence of $\text{Cs}_2\text{AgInCl}_6$, $\text{Cs}_2\text{NaInCl}_6$
8 and $\text{Cs}_2\text{Na}_{0.4}\text{Ag}_{0.6}\text{InCl}_6$. (f) Transient absorption spectra for $\text{Cs}_2\text{Ag}_{0.6}\text{Na}_{0.4}\text{InCl}_6$.
9 $\Delta A/A$ is the optical density. (g) Emission intensity versus excitation power for
10 $\text{Cs}_2\text{Ag}_{0.6}\text{Na}_{0.4}\text{InCl}_6$. Panels b-g are reprinted from ref 26 with permission from
11 Springer Nature.

12
13
14 In our previous work we found double perovskite $\text{Cs}_2\text{AgInCl}_6$ exhibits a
15 warm-white emission spectrum from 400 nm to 800 nm.⁴⁶ Besides the main
16 broad peak at 590 nm, a weak peak shows up at 430 nm (Figure 4a), which
17 may be attributed to FE emission. The lifetimes of two peaks are also in
18 agreement with FE and STE emission.⁴⁶ Simultaneous emission of FE and STE
19 is the feature of 2D and 3D perovskites with STE emission, which has been
20 discussed before. Theoretical calculation revealed that due to the delocalized In

1
2
3
4 5s states, the wave function of electrons is dispersive and has a 3D structure,
5
6
7 while the holes are confined at [AgCl₆] with a 0D structure (Figure 4b).²⁶ After
8
9
10 excitation, holes will be partially trapped at Ag atoms quickly and change the
11
12
13 electronic configuration from 4d¹⁰ to 4d⁹, favoring a Jahn-Teller distortion and
14
15
16 further resulting in the STE formation as the process in the formation of STE in
17
18
19 AgCl.²⁶ FE emission still present in Cs₂AgInCl₆, in analogy with 2D or 3D
20
21
22 hybrid halide perovskites, enabling potential white emission. We obtained the
23
24
25 Huang-Rhys factor in Cs₂AgInCl₆ with theoretical value 37 and experimental
26
27
28 value 38.7.²⁶ This is an appropriate value for efficient emission but the PLQY
29
30
31 of Cs₂AgInCl₆ is extremely low (<0.1%). One reason is that the FE and STE
32
33
34 are parity-forbidden transition. Another reason is small overlap between the
35
36
37 wave function distributions of electrons and holes (Figure 4b).²⁶ All in all,
38
39
40 Cs₂AgInCl₆ is a promising white emission material as long as these two
41
42
43
44
45
46
47 problems are overcome.
48
49
50

51 Recently we made a breakthrough by Na alloying Cs₂AgInCl₆. Parity-
52
53
54 forbidden transition derives from the inversion symmetry of the crystal structure
55
56
57
58
59
60

1
2
3 in $\text{Cs}_2\text{AgInCl}_6$.⁴⁷ Thereby we proposed that the parity-forbidden property could
4
5
6 be removed as long as the inversion symmetry was broken, for example, via
7
8
9 partial substitution to Ag. Alkali metal has a distinctively different electronic
10
11
12 configuration to Ag and thus is an appropriate candidate. In addition,
13
14
15
16 $\text{Cs}_2\text{AgInCl}_6$ and $\text{Cs}_2\text{NaInCl}_6$ have the same crystal structure and a negligible
17
18
19 lattice mismatch (0.3%).²⁶ We thus anticipated, and experimentally validated,
20
21
22 that there would not be detrimental defects or phase separation when Na was
23
24
25 introduced into $\text{Cs}_2\text{AgInCl}_6$. Theoretical calculation revealed that in $\text{Cs}_2\text{Na}_x\text{Ag}_{1-x}$
26
27
28 InCl_6 , the STE is spatially confined by Na^+ , leading to enhanced electron and
29
30
31 hole orbital overlap (Figure 4d).²⁶ The inversion symmetry of the $\text{Cs}_2\text{AgInCl}_6$ is
32
33
34 also broken upon Na alloying (Figure 4c). These two factors combined resulted
35
36
37 in the improvement of luminescence intensity by 3 order of magnitude.
38
39
40
41
42
43 Experimental evidence for the decreased electronic dimensionality is that
44
45
46 contrast to the origin $\text{Cs}_2\text{AgInCl}_6$, Na alloyed $\text{Cs}_2\text{AgInCl}_6$ exhibits an evident
47
48
49 exciton absorption peak at 365nm (Figure 4e). Na alloying also raised the
50
51
52 activation energy and decomposition temperature, and thus helping the emission
53
54
55
56
57
58
59
60

1
2
3 stability. Trace Bi^{3+} was further introduced to diminish defects in $\text{Cs}_2\text{Na}_x\text{Ag}_{1-x}\text{InCl}_6$
4
5
6
7 and depress the non-radiative recombination and further enhance PLQY
8
9
10 to 86% (peak value, 70% for average value), an unprecedented emission
11
12
13 efficiency for white emissive phosphors.
14
15
16
17

18 In addition, STE emission is also observed in double perovskites
19
20
21 nanocrystals. Manna et al. first reported $\text{Cs}_2\text{AgInCl}_6$ nanocrystals with white
22
23
24 emission (1.6% PLQY)⁴⁸, which exhibited good stability under air. Han et al.
25
26
27 also reported a bright dual-color emission in $\text{Cs}_2\text{AgBi}_x\text{In}_{1-x}\text{Cl}_6$ double perovskite
28
29
30 nanocrystals⁴⁹, which is similar with the STE emission mechanism in
31
32
33
34 $\text{Cs}_2\text{Na}_x\text{Ag}_{1-x}\text{InCl}_6$ bulk materials. Moreover, self-trapping process is also
35
36
37
38 observed in some new perovskite nanocrystals that have not been reported for
39
40
41 the bulk form, such as $\text{Cs}_2\text{AgSb}_x\text{In}_{1-x}\text{Br}_6$ ⁵⁰. Thus STEs in halide perovskites
42
43
44
45 nanocrystals deserve further researches to deepen the understanding and
46
47
48 realize its full potential.
49
50
51

52 The STEs and defects are apparently similar in many ways; however the crucial
53
54 difference is that the ground state of STE is actually the perfect lattice.⁴ After the free carriers
55
56
57
58
59
60

1
2
3 generated, the lattice will quickly distort and STE will form simultaneously. Generally, the
4
5 exciton self-trapping time should be comparable to the vibrational period of this phonon mode.
6
7 Hence the time can be evaluated as $\tau=2\pi/\Omega$ (Ω is phonon energy). This estimated time is about
8
9 several hundred femtoseconds and has been demonstrated experimentally by transient absorption
10
11 (Figure 4f).^{23, 26} Another accessible experimental evidence is the emission intensity has a
12
13 linear relationship with excitation power (Figure 4g).²⁶ That is because the
14
15 defects emission is easier to be saturated under high excitation power. Other
16
17 discernable evidence for the STE emission include similar photoluminescence
18
19 excitation spectrum and photoluminescence lifetimes for emitted photons of
20
21 different wavelength, and photo-introduced absorption in the transient absorption
22
23 spectrum²⁶.
24
25
26
27
28
29
30
31
32
33
34
35
36
37
38
39
40
41
42
43
44
45
46
47
48
49
50
51
52
53
54
55
56
57
58
59
60

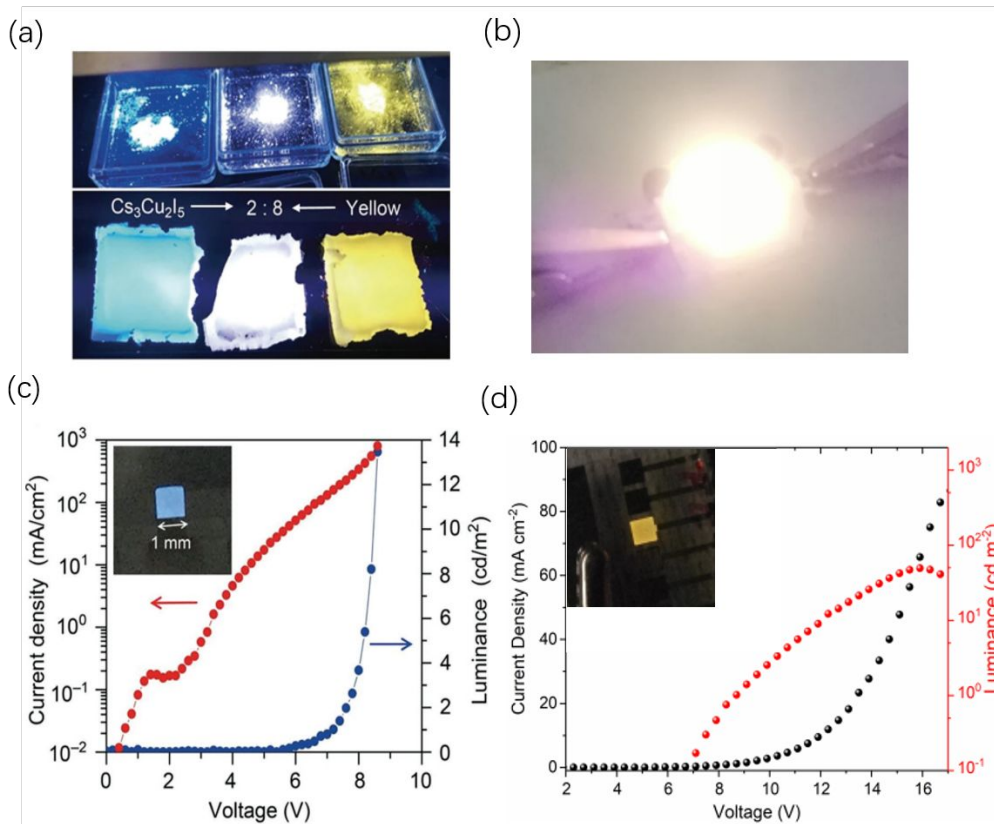


Figure 5. (a) The photograph of Cs₃Cu₂I₅ and yellow phosphor and their mixture at the ratio of 2:8 under ultraviolet (UV) light. Reprinted from ref 25 with permission from John Wiley & Sons Ltd. (b) The down-conversion light-emitting-diode (LED) based on Cs₂Na_{0.4}Ag_{0.6}InCl₆ phosphor. (c) The current-density-luminescence-voltage curves of Cs₃Cu₂I₅ LED. The inset shows the LED device while working. Reprinted from ref 25 with permission from John Wiley & Sons Ltd. (d) The current-density-luminescence-voltage curves of Cs₂Na_{0.4}Ag_{0.6}InCl₆ LED. The

1
2
3 inset shows the LED device while working. Reprinted from ref 26 with
4
5
6
7 permission from Springer Nature.
8
9

10
11 For phosphors applied in general lighting, broad spectrum is required to
12
13
14 achieve a high color rendering index (CRI), which is an important indicator for
15
16
17 light source to reveal the colors of various objects faithfully.⁵¹ And large stokes-
18
19
20 shift promises a negligible self-absorption, as self-absorption could seriously
21
22
23 restrict the total efficiency of the LED.⁵² Accordingly, efficient STE emitters are
24
25
26 ideal phosphors used in general lighting. White phosphor based on a mixture of
27
28
29 $\text{Cs}_3\text{Cu}_2\text{I}_5$ and yellow phosphor was demonstrated and showed a good
30
31
32 performance (Figure 5a).²⁵ We also demonstrated a warm white light emitting
33
34
35 diode with one single phosphor based on the optimized $\text{Cs}_2\text{Na}_x\text{Ag}_{1-x}\text{InCl}_6$
36
37
38 (Figure 5b).²⁶ Benefiting from the large exciton binding energy and the high
39
40
41 light and thermal stability of double perovskite, the phosphor shows no obvious
42
43
44 variation for the spectrum or the intensity, when operating at 333 K, or heated
45
46
47 at a 150 °C for 1000 hours, or working at 5000 cd/m² for 1000 hours.²⁶ These
48
49
50
51
52
53
54
55
56
57
58
59
60

1
2
3 positive results probably promise a huge market prospect for high efficient STE
4
5
6
7 emitters.
8
9

10
11 For lighting applications, the phosphors are generally excited by an
12
13 electrically pumped light emitting diodes (LEDs). Hence besides a high PLQY, it
14
15 is necessary for the optimum excitation wavelength to match this range for STE
16
17 emitter to achieve high power efficiency. Current III-Nitride based UV LEDs
18
19 shows excellent performance in the range of 365 nm~400 nm, yet substantially
20
21 lower efficiency below 365 nm.⁵³ The optimum excitation wavelength of
22
23 $\text{Cs}_2\text{Na}_x\text{Ag}_{1-x}\text{InCl}_6$ is on the boundary of this range²⁶ (exactly at 365 nm, Figure
24
25 4e), but those of $\text{Cs}_3\text{Cu}_2\text{I}_5$ and Cs_4SnBr_6 are out of this range²⁴⁻²⁵ (Figure 3f
26
27 and 3b). To reduce the overly large stokes shift, one possible solution is to
28
29 explore other element alloying or substitution to minimize the lattice deformation
30
31 energy E_d and self-trapped energy E_{St} .
32
33
34
35
36
37
38
39
40
41
42
43
44
45
46
47
48

49 It would be scientifically interesting and technologically attractive to
50
51 directly make electroluminescent (EL) devices using STE material as the
52
53
54
55
56
57
58
59
60

1
2
3 emission layer. Though many lead and tin halide perovskites with efficient STE
4
5
6
7 emission have been discovered, few STE emission based EL study is reported.
8
9
10 One possible reason is the large organic group severely impedes the transport
11
12
13 of carriers, and the tremendous heat released during working might destroy the
14
15
16 materials themselves. However, this problem can be resolved to a great extent
17
18
19 via using all-inorganic STE emitter. EL devices based on both of $\text{Cs}_3\text{Cu}_2\text{I}_5$ and
20
21
22 $\text{Cs}_2\text{Na}_x\text{Ag}_{1-x}\text{InCl}_6$ have been reported²⁵⁻²⁶ (Figure 5c and 5d). As expected, the
23
24
25
26
27 EL devices emit similar spectra with their PL spectra. Nevertheless, both of
28
29
30 them have a large threshold voltage and low efficiency. There are two main
31
32
33 obstacles: the low carrier mobility because of their low electronic dimensionality
34
35
36 and strong coupling to the lattice, and the poor charge injection due to their
37
38
39 large bandgap. Overall, both are fundamental challenges and we believe there
40
41
42
43
44 remains a long way for STE EL device to realize their full potential.
45
46
47
48
49
50
51
52
53
54
55
56
57
58
59
60

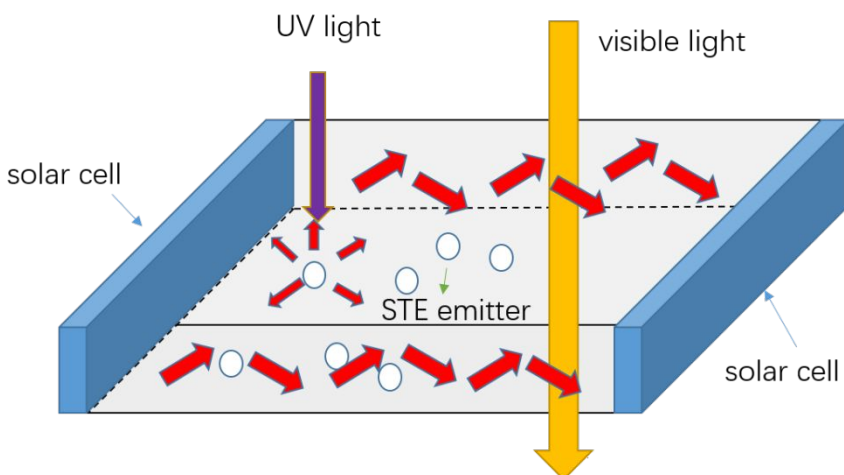


Figure 6. Schematic of luminescent solar concentrator based on STE emitter.

Considering the high PLQY and large stokes-shift, we propose that these STE emitters could be promising for luminescent solar concentrators (LSCs).⁵⁴⁻⁵⁹

LSCs are a potential approach to decrease the usage of traditional solar cells by concentrating solar irradiation through luminescent materials (Figure 6).

There are mainly two kinds of phosphors used in LSCs: fluorescent dyes and quantum dots (QDs).⁵⁹ Fluorescent dyes have large stokes-shift but their stability under long time illumination is unsatisfactory. Quantum dots can have a near-unity PLQY and a good light stability; however, large stoke-shift have to be judiciously engineered⁵⁷ (for example, giant shells) and their high-cost

1
2
3 synthesis is also a concern. STE emitters, particularly $\text{Cu}_3\text{Cu}_2\text{I}_5$ and $\text{Cs}_2\text{Na}_x\text{Ag}_{1-x}\text{InCl}_6$,
4
5
6
7
8
9
10
11
12
13
14
15
16
17
18
19
20
21
22
23
24
25
26
27
28
29
30
31
32
33
34
35
36
37
38
39
40
41
42
43
44
45
46
47
48
49
50
51
52
53
54
55
56
57
58
59
60
synthesis is also a concern. STE emitters, particularly $\text{Cu}_3\text{Cu}_2\text{I}_5$ and $\text{Cs}_2\text{Na}_x\text{Ag}_{1-x}\text{InCl}_6$, combine the advantages of high PLQY, good thermal stability, large stokes shift with minimized self-absorption, and low-cost manufacturing. Solar windows using these STE emitters further enjoy high transparency, an important feature for windows.⁵⁸ The shortcoming is these materials often only absorb the UV portion of solar spectrum, thus suffering from low efficiency.

In conclusion, STE derives from large electron-phonon coupling and soft lattice and is featured with broad spectrum and large stokes-shift, making it somewhat peculiar compared with other intrinsic luminescence. 2D hybrid perovskites have co-existence of FE and STE and hence high quality white emission but the obvious setback is low PLQY; 0D hybrid perovskites have a near-unity PLQY but lose the FE component and white emission. The thermal instability brought by organic groups could be improved by the all-inorganic perovskite counterparts. Cs_4SnBr_6 , $\text{Cs}_3\text{Cu}_2\text{I}_5$ and $\text{Cs}_2\text{AgInCl}_6$ are such three prominent examples. Particularly for $\text{Cs}_2\text{AgInCl}_6$, through Na alloying to break the parity forbidden transition and reduce the electronic dimensionality and

1
2
3 through Bi^{3+} doping to suppress non-radiative defects, the optimized white
4
5
6 emissive $\text{Cs}_2\text{Na}_{0.4}\text{Ag}_{0.6}\text{InCl}_6$ STE emitters combines outstanding PLQY and
7
8
9 excellent thermal, air and light stability and shows promise as down conversion
10
11
12 phosphors for solid state lighting .
13
14
15

16
17
18 The study of STE emission in halide perovskites or related variants are
19
20 only at their infancy stage; there remain a large room to be explored. Instead
21
22 of V_k center in alkali halides, Jahn-Teller distortion in octahedra favors the
23
24 formation of STE in halide perovskites. Further understanding of the lattice
25
26 distortion process, the decay pathway of STE emission, as well as other
27
28 relevant mechanism are urgent. Furthermore, all-inorganic perovskites with
29
30 efficient STE emission are scarce contrast to various organic STE emitting
31
32 perovskites. Synthesizing new all-inorganic materials with efficient STE emission
33
34 and preferably high quality white emission with >365 nm excitation is of great
35
36 significance. So far, the seemly promising application for STE emitting
37
38 perovskites is phosphor used in general lighting. Therefore exploring new
39
40 applications, for example, luminescent solar concentrators, is very meaningful.
41
42
43
44
45
46
47
48
49
50
51
52
53
54
55
56
57
58
59
60

1
2
3
4
5
6
7 **AUTHOR INFORMATION**
8
9

10 **Corresponding Author**
11
12

13
14 *E-mail: jtang@mail.hust.edu.cn (J.T)
15
16

17
18 **ORCID**
19
20

21
22 Jiang Tang: 0000-0003-2574-2943
23
24

25
26 **Author Contributions**
27
28

29 ‡ S.L and J.L contributed equally to this work.
30
31

32
33 **Notes**
34
35

36
37 The authors declare no competing financial interests.
38
39

40
41 **ACKNOWLEDGMENTS**
42
43

44
45 This work was financially supported by the National Natural Science Foundation
46
47
48
49 of China (5171101030 and 61725401), the National Key R&D Program of China
50
51

(2016YFB0700702), and the HUST Key Innovation Team for Interdisciplinary Promotion (2016JCTD111 and 2017KFXKJC003).

REFERENCES

- (1) Vij, D. *Luminescence of Solids*. Springer Science & Business Media: New York, 2012.
- (2) Schubert, E. F. *Light-Emitting Diodes*. E. Fred Schubert: New York, 2018.
- (3) Van Eijk, C. Cross-luminescence. *J. Lumin.* **1994**, *60*, 936-941.
- (4) Song, K.; Williams, R. T. *Self-Trapped Excitons*. Springer Science & Business Media: Berlin, 2013; Vol. 105.
- (5) Williams, R. T.; Song, K. S.; Faust, W. L.; Leung, C. H. Off-center self-trapped excitons and creation of lattice defects in alkali halide crystals. *Phys. Rev. B* **1986**, *33*, 7232-7240.
- (6) Fowler, W. B.; Marrone, M. J.; Kabler, M. N. Theory of Self-Trapped Exciton Luminescence in Halide Crystals. *Phys. Rev. B* **1973**, *8*, 5909-5919.
- (7) Menzel, D. Valence and core excitations in rare gas mono- and multilayers: Production, decay, and desorption of neutrals and ions. *Appl. Phys. A* **1990**, *51*, 163-171.
- (8) Scholz, R.; Kobitski, A. Y.; Zahn, D. R. T.; Schreiber, M. Investigation of molecular dimers in α -PTCDA by ab initio methods: Binding energies, gas-to-crystal shift, and self-trapped excitons. *Phys. Rev. B* **2005**, *72*, 245208.
- (9) Chen, Y.; Duh, J.; Chiou, B.; Peng, C. Luminescent mechanisms of ZnS:Cu:Cl and ZnS:Cu:Al phosphors. *Thin Solid Films* **2001**, *392*, 50-55.
- (10) Stadler, W.; Hofmann, D. M.; Alt, H. C.; Muschik, T.; Meyer, B. K.; Weigel, E.; Müller-Vogt, G.; Salk, M.; Rupp, E.; Benz, K. W. Optical investigations of defects in $\text{Cd}_{1-x}\text{Zn}_x\text{Te}$. *Phys. Rev. B* **1995**, *51*, 10619-10630.
- (11) Barkaoui, H.; Abid, H.; Yangui, A.; Triki, S.; Boukheddaden, K.; Abid, Y. Yellowish White-Light Emission Involving Resonant Energy Transfer in a New

1
2
3
4 One-Dimensional Hybrid Material: $(C_9H_{10}N_2)PbCl_4$. *J. Phys. Chem. C* **2018**, *122*,
5 24253-24261.

6
7 (12) Wang, S.; Yao, Y.; Wu, Z.; Peng, Y.; Li, L.; Luo, J. Realization of “warm”
8 white light via halide substitution in polar two-dimensional hybrid perovskites
9 $(2mepH_2)PbCl_xBr_{4-x}$. *J. Mater. Chem. C* **2018**, *6*, 12267-12272.

10
11 (13) Zhou, C.; Lin, H.; Worku, M.; Neu, J.; Zhou, Y.; Tian, Y.; Lee, S.;
12 Djurovich, P.; Siegrist, T.; Ma, B. Blue Emitting Single Crystalline Assembly of
13 Metal Halide Clusters. *J. Am. Chem. Soc.* **2018**, *140*, 13181-13184.

14
15 (14) Mao, L.; Wu, Y.; Stoumpos, C. C.; Traore, B.; Katan, C.; Even, J.;
16 Wasielewski, M. R.; Kanatzidis, M. G. Tunable White-Light Emission in Single-
17 Cation-Templated Three-Layered 2D Perovskites $(CH_3CH_2NH_3)_4Pb_3Br_{10-x}Cl_x$. *J.*
18 *Am. Chem. Soc.* **2017**, *139*, 11956-11963.

19
20 (15) Dohner, E. R.; Jaffe, A.; Bradshaw, L. R.; Karunadasa, H. I. Intrinsic
21 white-light emission from layered hybrid perovskites. *J. Am. Chem. Soc.* **2014**,
22 *136*, 13154-13157.

23
24 (16) Dohner, E. R.; Hoke, E. T.; Karunadasa, H. I. Self-assembly of
25 broadband white-light emitters. *J. Am. Chem. Soc.* **2014**, *136*, 1718-1721.

26
27 (17) Zhou, C.; Worku, M.; Neu, J.; Lin, H.; Tian, Y.; Lee, S.; Zhou, Y.; Han,
28 D.; Chen, S.; Hao, A.; et al. Facile Preparation of Light Emitting Organic Metal
29 Halide Crystals with Near-Unity Quantum Efficiency. *Chem. Mater.* **2018**, *30*,
30 2374-2378.

31
32 (18) Smith, M. D.; Watson, B. L.; Dauskardt, R. H.; Karunadasa, H. I.
33 Broadband Emission with a Massive Stokes Shift from Sulfonium Pb-Br Hybrids.
34 *Chem. Mater.* **2017**, *29*, 7083-7087.

35
36 (19) Zhou, C.; Lin, H.; Tian, Y.; Yuan, Z.; Clark, R.; Chen, B.; van de Burgt,
37 L. J.; Wang, J. C.; Zhou, Y.; Hanson, K.; et al. Luminescent zero-dimensional
38 organic metal halide hybrids with near-unity quantum efficiency. *Chem. Sci.*
39 **2018**, *9*, 586-593.

40
41 (20) Zhou, C.; Tian, Y.; Wang, M.; Rose, A.; Besara, T.; Doyle, N. K.; Yuan,
42 Z.; Wang, J. C.; Clark, R.; Hu, Y.; et al. Low-Dimensional Organic Tin Bromide
43 Perovskites and Their Photoinduced Structural Transformation. *Angew. Chem.*
44 *Int. Ed.* **2017**, *56*, 9018-9022.

- 1
2
3
4 (21) Hu, T.; Smith, M. D.; Dohner, E. R.; Sher, M. J.; Wu, X.; Trinh, M. T.;
5 Fisher, A.; Corbett, J.; Zhu, X. Y.; Karunadasa, H. I.; et al. Mechanism for
6 Broadband White-Light Emission from Two-Dimensional (110) Hybrid
7 Perovskites. *J. Phys. Chem. Lett.* **2016**, *7*, 2258-2263.
8
9
10 (22) Smith, M. D.; Jaffe, A.; Dohner, E. R.; Lindenberg, A. M.; Karunadasa,
11 H. I. Structural origins of broadband emission from layered Pb-Br hybrid
12 perovskites. *Chem. Sci.* **2017**, *8*, 4497-4504.
13
14
15 (23) Smith, M. D.; Karunadasa, H. I. White-Light Emission from Layered
16 Halide Perovskites. *Acc. Chem. Res.* **2018**, *51*, 619-627.
17
18
19 (24) Benin, B. M.; Dirin, D. N.; Morad, V.; Wörle, M.; Yakunin, S.; Rainò, G.;
20 Nazarenko, O.; Fischer, M.; Infante, I.; Kovalenko, M. V. Highly Emissive Self-
21 Trapped Excitons in Fully Inorganic Zero-Dimensional Tin Halides. *Angew.*
22 *Chem. Int. Ed.* **2018**, *57*, 11329-11333.
23
24
25 (25) Jun, T.; Sim, K.; Imura, S.; Sasase, M.; Kamioka, H.; Kim, J.; Hosono,
26 H. Lead-Free Highly Efficient Blue-Emitting Cs₃Cu₂I₅ with 0D Electronic
27 Structure. *Adv. Mater.* **2018**, *30*, 1804547.
28
29
30 (26) Luo, J.; Wang, X.; Li, S.; Liu, J.; Guo, Y.; Niu, G.; Yao, L.; Fu, Y.; Gao,
31 L.; Dong, Q.; et al. Efficient and stable emission of warm-white light from lead-
32 free halide double perovskites. *Nature* **2018**, *563*, 541-545.
33
34
35 (27) Fu, P.; Huang, M.; Shang, Y.; Yu, N.; Zhou, H. L.; Zhang, Y. B.; Chen,
36 S.; Gong, J.; Ning, Z. Organic-Inorganic Layered and Hollow Tin Bromide
37 Perovskite with Tunable Broadband Emission. *ACS Appl. Mater. Interfaces*
38 **2018**, *10*, 34363-34369.
39
40
41
42 (28) Tomimoto, S.; Nansei, H.; Saito, S.; Suemoto, T.; Takeda, J.; Kurita, S.
43 Femtosecond dynamics of the exciton self-trapping process in a quasi-one-
44 dimensional halogen-bridged platinum complex. *Phys. Rev. Lett.* **1998**, *81*, 417-
45 420.
46
47
48
49 (29) Wada, Y.; Lemmer, U.; Göbel, E. O.; Yamashita, M.; Toriumi, K. Time-
50 resolved luminescence study of self-trapped-exciton relaxation in quasi-one-
51 dimensional halogen-bridged mixed-valence metal complexes. *Phys. Rev. B*
52 **1995**, *52*, 8276-8282.
53
54
55
56
57
58
59
60

- 1
2
3
4 (30) Suemoto, T.; Tomimoto, S. Femtosecond dynamics of self-trapped
5 excitons in quasi-one-dimensional halogen-bridged Pt complexes. *J. Lumin.*
6 **1999**, *83*, 13-18.
7
8 (31) Emin, D.; Holstein, T. Adiabatic Theory of an Electron in a Deformable
9 Continuum. *Phys. Rev. Lett.* **1976**, *36*, 323-326.
10
11 (32) Kabanov, V. V.; Mashtakov, O. Y. Electron localization with and without
12 barrier formation. *Phys. Rev. B* **1993**, *47*, 6060-6064.
13
14 (33) Hayashi, T.; Kobayashi, T.; Iwanaga, M.; Watanabe, M. Exciton dynamics
15 related with phase transitions in CsPbCl₃ single crystals. *J. Lumin.* **2001**, *94*,
16 255-259.
17
18 (34) Zhang, D.; Eaton, S. W.; Yu, Y.; Dou, L.; Yang, P. Solution-Phase
19 Synthesis of Cesium Lead Halide Perovskite Nanowires. *J. Am. Chem. Soc.*
20 **2015**, *137*, 9230-9233.
21
22 (35) Xiao, Z.; Meng, W.; Wang, J.; Mitzi, D. B.; Yan, Y. Searching for
23 promising new perovskite-based photovoltaic absorbers: The importance of
24 electronic dimensionality. *Mater. Horiz.* **2017**, *4*, 206-216.
25
26 (36) Wei, F.; Deng, Z.; Sun, S.; Xie, F.; Kieslich, G.; Evans, D. M.; Carpenter,
27 M. A.; Bristowe, P. D.; Cheetham, A. K. The synthesis, structure and electronic
28 properties of a lead-free hybrid inorganic-organic double perovskite (MA)₂KBiCl₆
29 (MA = methylammonium). *Mater. Horiz.* **2016**, *3*, 328-332.
30
31 (37) Volonakis, G.; Filip, M. R.; Haghighirad, A. A.; Sakai, N.; Wenger, B.;
32 Snaith, H. J.; Giustino, F. Lead-Free Halide Double Perovskites via Heterovalent
33 Substitution of Noble Metals. *J. Phys. Chem. Lett.* **2016**, *7*, 1254-1259.
34
35 (38) Filip, M. R.; Hillman, S.; Haghighirad, A. A.; Snaith, H. J.; Giustino, F.
36 Band Gaps of the Lead-Free Halide Double Perovskites Cs₂BiAgCl₆ and
37 Cs₂BiAgBr₆ from Theory and Experiment. *J. Phys. Chem. Lett.* **2016**, *7*, 2579-
38 2585.
39
40 (39) Zhao, X. G.; Yang, J. H.; Fu, Y.; Yang, D.; Xu, Q.; Yu, L.; Wei, S. H.;
41 Zhang, L. Design of Lead-Free Inorganic Halide Perovskites for Solar Cells via
42 Cation-Transmutation. *J. Am. Chem. Soc.* **2017**, *139*, 2630-2638.
43
44
45
46
47
48
49
50
51
52
53
54
55
56
57
58
59
60

- 1
2
3
4 (40) Slavney, A. H.; Hu, T.; Lindenberg, A. M.; Karunadasa, H. I. A Bismuth-
5 Halide Double Perovskite with Long Carrier Recombination Lifetime for
6 Photovoltaic Applications. *J. Am. Chem. Soc.* **2016**, *138*, 2138-2141.
- 7
8 (41) Wei, F.; Deng, Z.; Sun, S.; Zhang, F.; Evans, D. M.; Kieslich, G.;
9 Tominaka, S.; Carpenter, M. A.; Zhang, J.; Bristowe, P. D.; et al. Synthesis and
10 Properties of a Lead-Free Hybrid Double Perovskite: $(\text{CH}_3\text{NH}_3)_2\text{AgBiBr}_6$. *Chem.*
11 *Mater.* **2017**, *29*, 1089-1094.
- 12
13 (42) McClure, E. T.; Ball, M. R.; Windl, W.; Woodward, P. M. $\text{Cs}_2\text{AgBiX}_6$ (X =
14 Br, Cl): New Visible Light Absorbing, Lead-Free Halide Perovskite
15 Semiconductors. *Chem. Mater.* **2016**, *28*, 1348-1354.
- 16
17 (43) Du, K. Z.; Meng, W.; Wang, X.; Yan, Y.; Mitzi, D. B. Bandgap
18 Engineering of Lead-Free Double Perovskite $\text{Cs}_2\text{AgBiBr}_6$ through Trivalent Metal
19 Alloying. *Angew. Chem. Int. Ed.* **2017**, *56*, 8158-8162.
- 20
21 (44) Savory, C. N.; Walsh, A.; Scanlon, D. O. Can Pb-Free Halide Double
22 Perovskites Support High-Efficiency Solar Cells? *ACS Energy Lett.* **2016**, *1*,
23 949-955.
- 24
25 (45) Zhao, X.-G.; Yang, D.; Ren, J.-C.; Sun, Y.; Xiao, Z.; Zhang, L. Rational
26 Design of Halide Double Perovskites for Optoelectronic Applications. *Joule*
27 **2018**, *2*, 1662-1673.
- 28
29 (46) Luo, J.; Li, S.; Wu, H.; Zhou, Y.; Li, Y.; Liu, J.; Li, J.; Li, K.; Yi, F.; Niu,
30 G.; Tang, J. $\text{Cs}_2\text{AgInCl}_6$ Double Perovskite Single Crystals: Parity Forbidden
31 Transitions and Their Application For Sensitive and Fast UV Photodetectors.
32 *ACS Photonics* **2017**, *5*, 398-405.
- 33
34 (47) Meng, W.; Wang, X.; Xiao, Z.; Wang, J.; Mitzi, D. B.; Yan, Y. Parity-
35 Forbidden Transitions and Their Impact on the Optical Absorption Properties of
36 Lead-Free Metal Halide Perovskites and Double Perovskites. *J. Phys. Chem.*
37 *Lett.* **2017**, *8*, 2999-3007.
- 38
39 (48) Locardi, F.; Cirignano, M.; Baranov, D.; Dang, Z.; Prato, M.; Drago, F.;
40 Ferretti, M.; Pinchetti, V.; Fanciulli, M.; Brovelli, S.; et al. Colloidal Synthesis of
41 Double Perovskite $\text{Cs}_2\text{AgInCl}_6$ and Mn-Doped $\text{Cs}_2\text{AgInCl}_6$ Nanocrystals. *J. Am.*
42 *Chem. Soc.* **2018**, *140*, 12989-12995.
- 43
44
45
46
47
48
49
50
51
52
53
54
55
56
57
58
59
60

- 1
2
3
4 (49) Yang, B.; Mao, X.; Hong, F.; Meng, W.; Tang, Y.; Xia, X.; Yang, S.;
5 Deng, W.; Han, K. Lead-Free Direct Bandgap Double Perovskite Nanocrystals
6 with Bright Dual-Color Emission. *J. Am. Chem. Soc.* **2018**, *140*, 17001-17006.
7
8 (50) Han, K.; Yang, B.; Hong, F.; Chen, J.; Tang, Y.; Yang, L.; Sang, Y.; Xia,
9 X.; Guo, J.; He, H. Colloidal Synthesis and Charge-Carrier Dynamics of
10 $\text{Cs}_2\text{AgSb}_{1-y}\text{Bi}_y\text{X}_6$ (X: Br, Cl; $0 \leq y \leq 1$) Double Perovskite Nanocrystals. *Angew.*
11 *Chem. Int. Ed.* **2018**. DOI: 10.1002/anie.201811610
12
13 (51) Wang, L.; Xie, R. J.; Suehiro, T.; Takeda, T.; Hirosaki, N. Down-
14 Conversion Nitride Materials for Solid State Lighting: Recent Advances and
15 Perspectives. *Chem. Rev.* **2018**, *118*, 1951-2009.
16
17 (52) Shang, M.; Li, C.; Lin, J. How to produce white light in a single-phase
18 host? *Chem. Soc. Rev.* **2014**, *43*, 1372-1386.
19
20 (53) Kneissl, M.; Rass, J. III-Nitride ultraviolet emitters. In *Springer Series in*
21 *Materials Science*, Springer: Heidelberg, 2016.
22
23 (54) Van Sark, W. G.; Barnham, K. W.; Slooff, L. H.; Chatten, A. J.;
24 Büchtemann, A.; Meyer, A.; McCormack, S. J.; Koole, R.; Farrell, D. J.; Bose,
25 R. Luminescent solar concentrators: A review of recent results. *Opt. Express*
26 **2008**, *16*, 21773-21792.
27
28 (55) Batchelder, J.; Zewai, A.; Cole, T. Luminescent solar concentrators. 1:
29 Theory of operation and techniques for performance evaluation. *Appl. Optics*
30 **1979**, *18*, 3090-3110.
31
32 (56) Bergren, M. R.; Makarov, N. S.; Ramasamy, K.; Jackson, A.; Guglielmetti,
33 R.; McDaniel, H. High-Performance CuInS_2 Quantum Dot Laminated Glass
34 Luminescent Solar Concentrators for Windows. *ACS Energy Lett.* **2018**, *3*, 520-
35 525.
36
37 (57) Meinardi, F.; Colombo, A.; Velizhanin, K. A.; Simonutti, R.; Lorenzon, M.;
38 Beverina, L.; Viswanatha, R.; Klimov, V. I.; Brovelli, S. Large-area luminescent
39 solar concentrators based on 'Stokes-shift-engineered' nanocrystals in a mass-
40 polymerized PMMA matrix. *Nat. Photonics* **2014**, *8*, 392-399.
41
42 (58) Zhao, Y.; Lunt, R. R. Transparent Luminescent Solar Concentrators for
43 Large-Area Solar Windows Enabled by Massive Stokes-Shift Nanocluster
44 Phosphors. *Adv. Energy Mater.* **2013**, *3*, 1143-1148.
45
46
47
48
49
50
51
52
53
54
55
56
57
58
59
60

1
2
3
4 (59) Meinardi, F.; Bruni, F.; Brovelli, S. Luminescent solar concentrators for
5 building-integrated photovoltaics. *Nat. Rev. Mater.* **2017**, *2*, 17072.

6
7 (60) McCall, K. M.; Stoumpos, C. C.; Kostina, S. S.; Kanatzidis, M. G.;
8 Wessels, B. W. Strong Electron-Phonon Coupling and Self-Trapped Excitons in
9 the Defect Halide Perovskites $A_3M_2I_9$ (A = Cs, Rb; M = Bi, Sb). *Chem. Mater.*
10 **2017**, *29*, 4129-4145.
11
12
13
14
15
16
17
18
19
20
21
22
23
24
25
26
27
28
29
30
31
32
33
34
35
36
37
38
39
40
41
42
43
44
45
46
47
48
49
50
51
52
53
54
55
56
57
58
59
60